Received: 10 January 2024 | Accepted: 22 May 2024

DOI: 10.1002/jev2.12464

RESEARCH ARTICLE

AAV gene replacement therapy for treating MPS IIIC: Facilitating bystander effects via EV-mRNA cargo

Tierra A. Bobo[1,2] | **Michael Robinson**[1] | **Christopher Tofade**[1] | **Marina Sokolski-Papkov**[3] | **Peter Nichols**[1] | **Stephen Vorobiov**[1] | **Haiyan Fu**[1,2]

[1]Gene Therapy Center, Chapel Hill, USA

[2]Division of Genetics and Metabolism, Department of Pediatrics, School of Medicine, Chapel Hill, USA

[3]Center for Nanotechnology in Drug Delivery, Division of Molecular Pharmaceutics, Eshelman School of Pharmacy, University of North Carolina at Chapel Hill, Chapel Hill, USA

Correspondence
Tierra A. Bobo, Gene Therapy Center, Chapel Hill, USA.
Email: Tierra_Bobo@med.unc.edu

Funding information
North Carolina Biotechnology Center, Grant/Award Number: NCBC 2020-GTF-6903; National Institute of Neurological Disorders and Stroke, Grant/Award Number: R21NS118165; National Cancer Institute, Grant/Award Number: P30CA016086

Abstract

MPS IIIC is a lysosomal storage disease caused by mutations in heparan-α-glucosaminide *N*-acetyltransferase (HGSNAT), for which no treatment is available. Because HGSNAT is a trans-lysosomal-membrane protein, gene therapy for MPS IIIC needs to transduce as many cells as possible for maximal benefits. All cells continuously release extracellular vesicles (EVs) and communicate by exchanging biomolecules via EV trafficking. To address the unmet need, we developed a rAAV-hHGSNAT^{EV} vector with an EV-mRNA-packaging signal in the 3′UTR to facilitate bystander effects, and tested it in an in vitro MPS IIIC model. In human MPS IIIC cells, rAAV-hHGSNAT^{EV} enhanced HGSNAT mRNA and protein expression, EV-hHGSNAT-mRNA packaging, and cleared GAG storage. Importantly, incubation with EVs led to hHGSNAT protein expression and GAG contents clearance in recipient MPS IIIC cells. Further, rAAV-hHGSNAT^{EV} transduction led to the reduction of pathological EVs in MPS IIIC cells to normal levels, suggesting broader therapeutic benefits. These data demonstrate that incorporating the EV-mRNA-packaging signal into a rAAV-hHGSNAT vector enhances EV packaging of hHGSNAT-mRNA, which can be transported to non-transduced cells and translated into functional rHGSNAT protein, facilitating cross-correction of disease pathology. This study supports the therapeutic potential of rAAV^{EV} for MPS IIIC, and broad diseases, without having to transduce every cell.

KEYWORDS

adeno-associated virus (AAV), blood-brain-barrier, bystander effects/cross-correction, EV-mRNA cargo, lysosomal storage diseases, mucopolysaccharidosis type IIIC (MPS IIIC), rAAV gene therapy

1 | INTRODUCTION

Mucopolysaccharidosis (MPS) IIIC is a devastating ultra-rare neuropathic lysosomal storage disease (LSD), with an estimated incidence of 1 in 1,500,000 live births (Andrade et al., 2015). MPS IIIC is caused by autosomal recessive defects in the gene encoding heparan-α-glucosaminide *N*-acetyltransferase (HGSNAT). HGSNAT is one of the lysosomal enzymes involved in the degradation of heparan sulphate (HS), a class of biologically important glycosaminoglycans (GAGs), by catalysing acetylation of the non-reducing terminal α-glucosamine residue of HS. The lack of HGSNAT activity results in the accumulation HS-GAGs in the lysosomes in virtually all organs, especially in the nervous system, leading to severe progressive neuropathy. Infants with MPS IIIC appear normal at birth, but clinical manifestations emerge in early childhood with developmental delay and severe

neurological deterioration, leading to premature death before the 3rd decade (Andrade et al., 2015; Lavery et al., 2017). Somatic manifestations do occur in all individuals, though milder than other MPS disorders.

There is an urgent unmet medical need for patients with MPS IIIC, for which no treatments are currently available beyond case management and supportive care. Early findings revealed that the majority of lysosomal enzymes are secretory. The secreted enzymes can be taken up by neighboring cells and transported to lysosomes for metabolic function. This bystander effect has been the basis for hematopoietic stem cell transplantation (HSCT) and systemic enzyme replacement therapy (ERT), which are available for treating somatic disorders of some MPS diseases, such as MPS I, II and VI, but with no or limited neurological benefits (Andrade et al., 2015). MPS IIIC is not amenable to either HSCT or ERT, because HGSNAT is an exclusively transmembrane protein. Therefore, unlike most other lysosomal enzyme proteins, HGSNAT is not secreted and has no bystander effect, posing a particular challenge to therapeutic development.

Another challenge to therapeutic development for MPS IIIC is the presence of the blood-brain barrier (BBB) that prevent therapeutics from entering the CNS from the circulation (Duque et al., 2009; Fu et al., 2011; Hudry & Vandenberghe, 2019). Further, the pathology of MPS IIIC manifests in cells in virtually all organs, with global diffuse neuropathologies throughout the CNS and peripheral nervous system (PNS). Therefore, effective therapies for MPS IIIC require broad organ targeting, with global diffuse CNS delivery, which can be most effectively achieved by systemic delivery via the vascular route (Rapoport, 2000). This is also the case in the majority of neuropathic LSDs.

Gene replacement therapy (GRT), targeting the root cause of neuropathic LSDs provides an ideal treatment if delivered to broad CNS and peripheral tissues, because of the potential for long-term endogenous production of recombinant proteins. Recombinant adeno-associated viral (rAAV) vectors have been demonstrated to be promising solutions to these gene delivery challenges. AAV is a nonpathogenic, replication-defective parvovirus, with different AAV serotypes displaying broad tissue tropisms, and long-term expression in non-dividing cells of the CNS and periphery (Berns & Giraud, 1996; Fu et al., 2011). The demonstration of rAAV9 trans-BBB neurotropism has offered a potential solution for CNS gene delivery (Duque et al., 2009; Foust et al., 2009), leading to successes in developing treatments for neurogenetic diseases in animal models via systemic (Bevan et al., 2011; Bobo et al., 2020; Fu et al., 2011, 2016, 2018; Gross et al., 2022; Gurda et al., 2016; Lee et al., 2015; Ruzo et al., 2012; Weismann et al., 2015) or intrathecal (IT) delivery (Duque et al., 2015; Haurigot et al., 2013; Hinderer et al., 2014; Meyer et al., 2015; Mussche et al., 2013; Ribera et al., 2015). These efforts have led to the ground-breaking FDA approval of Zolgensma, a systemic rAAV9 gene replacement therapy for treating SMA1 (Mendell et al., 2017), and ongoing clinical trials for multiple neuropathic lysosomal storage diseases. Numerous studies also led to the IND approvals of IT AAV9 delivery for giant axonal neuropathy (Bailey et al., 2018), NCL3, NCL6, (Cain et al., 2019) MPS I (Hinderer et al., 2014) and MPS II (Hinderer et al., 2016). These successes strongly support the potential of gene replacement therapy using AAV9 for the effective treatment of other neurogenetic diseases, including MPS IIIC.

It is known that treating SMA with Zolgensma requires a substantially high dose (1.1×10^{14} vg/kg) for desired therapeutic benefits (Mendell et al., 2017). The high dose requirement is also the case in systemic GRT using different AAV serotypes, such as the recently approved ELEVIDYS for Duchene muscular dystrophy (DMD, 1.3×10^{14} vg/kg), and in ongoing clinical trials for XLMTM (AT132, $1–3.5 \times 10^{14}$ vg/kg), and DMD (RGX-202, $1–2 \times 10^{14}$ vg/kg). The requirement for high vector doses in treating these diseases, which all involve non-secreted proteins, is largely due to the necessity of transducing as many cells as possible to achieve significant benefits. This not only poses a critical challenge to the scale-up of rAAV manufacturing, but also the potential risk of severe toxicity. Severe acute adverse events have been reported in SMA1 patients treated with Zolgensma, and in an AAV gene therapy clinical trial for XLMTM. Notably, as shown in the preclinical studies leading to the approval of Zolgensma, the minimal effective dose (MED) of systemic scAAV9-SMN1 gene delivery was 6.6×10^{13} vg/kg (Foust et al., 2010). However, the MED for systemic scAAV9-h*SGSH* delivery was shown to be 5×10^{12} vg/kg for treating MPS IIIA (Fu et al., 2016), because SGSH is a secreted lysosomal enzyme protein that has natural bystander effects, which allow greater benefits via cross-correction, without the need to transduce every cell (Neufeld & Cantz, 1971).

All cell types are known to continuously release extracellular vesicles (EVs) to the extracellular environment, which can be found in the blood and virtually all body fluids. EVs are membrane-bound vesicles including plasma-membrane-derived microvesicles (100–500 nm) and exosomes of endocytic origin (50–150 nm) (Meldolesi, 2019, 2021; Urbanelli et al., 2016). EVs have been demonstrated to facilitate short- and long-distance intercellular communication and signalling to target recipient cells by all cell types (Meldolesi, 2019, 2021; Valadi et al., 2007). Interestingly, EVs carry lipids, proteins, peptides, mRNA, microRNAs (miRNAs), genomic DNA and mitochondrial DNA (Meldolesi, 2019, 2021; Urbanelli et al., 2016; Valadi et al., 2007). All cells are now known to communicate by the exchange of large molecules via EV traffic (Colombo et al., 2014; Meldolesi, 2019). Once released, EVs bind to neighbouring cells, or to the extracellular matrix, or traffic via the blood circulation or other body fluids before interacting with target cells. EVs participate in important biological functions as mediators of intercellular communication by adhering to the surface of recipient cells or being internalized by recipient cells, and releasing genetic content into recipient cells. (Belting & Wittrup, 2008; Mittelbrunn & Sánchez-Madrid, 2012; Vlassov et al., 2012) Once in the recipient cell, EV-transported RNAs are functional, as they would be in the originating source cells (Fatima & Nawaz, 2017; Hedlund et al., 2011; Li et al., 2013; Li et al., 2019; Montecalvo et al., 2012). Given that the EV 'cargo' can be delivered to other cells, loaded or

engineered EVs have been used as vehicles in drug delivery studies (Barile & Vassalli, 2017; Mizrak et al., 2013). Further, EVs have been linked to physiological and pathological conditions, such as autoimmune diseases including multiple sclerosis (MS) and cancer, in which increases in EV concentrations have been reported (Logozzi et al., 2009; Robbins & Morelli, 2014; Sáenz-Cuesta et al., 2014). EVs have been implicated in neurogenesis, synaptic activities, and normal functioning of the nervous system, and therefore have been used as vehicles in therapeutic studies for treating neurological diseases (de Jong et al., 2019; Gassama & Favereaux, 2021).

While the mechanisms governing how specific contents are packaged into EVs remain poorly understood, studies have shown that RNAs that are packaged in EVs include mRNA, miRNA, snRNA, lncRNA, rRNA, and tRNA (Lässer et al., 2017; Turchinovich et al., 2019). Studies by Bolukbasi *et al.* provide a clue as to how genetic materials are loaded into EVs, and identified a 25 nucleotide (nt) 'zip code' (ZC) sequence in the 3′UTR of mRNAs (Bolukbasi et al., 2012). Importantly, they demonstrated that the incorporation of this 25 nt sequence into the 3′UTR of a reporter gene in a plasmid led to the enrichment of reporter mRNA in EVs and significant increases in the reporter gene expression in recipient cells (Bolukbasi et al., 2012). Further, recent studies indicate that numerous RNA binding proteins (RBPs) are transported into EVs in association with RNA molecules in the form of RNA–RBP complexes with both cellular RNA and EV-RNA species (Kossinova et al., 2017; Shurtleff et al., 2017; Statello et al., 2018; Villarroya-Beltri et al., 2013; Wu et al., 2018; Yanshina et al., 2018). This type of association could be a general mechanism for RNA transport and maintenance into EVs, and may favor the shuttling of RNAs from EVs to recipient cells in the form of stable complexes (Kossinova et al., 2017; Shurtleff et al., 2017; Statello et al., 2018; Villarroya-Beltri et al., 2013; Wu et al., 2018; Yanshina et al., 2018). We therefore hypothesized that incorporating the EV-mRNA packaging signal sequences into rAAV gene therapy vectors could facilitate bystander effects of non-secreted proteins via AAV-expressed EV-mRNA cargo, offering greater therapeutic potential for gene therapies treating neurogenetic diseases involving non-secreted proteins, such as MPS IIIC.

To develop an effective rAAV9 GRT for treating MPS IIIC, in this study, we developed a rAAV vector containing the 25 nt EV-mRNA zip code sequence (Bolukbasi et al., 2012), linked to human HGSNAT (h*HGSNAT*) cDNA, to facilitate bystander effects. The rAAV-h*HGSNAT*^{EV} vector was tested in vitro in human MPS IIIC fibroblasts, and resulted in not only the expression of rHGSNAT protein, but also the release of hHGSNAT-mRNA-containing EVs. Importantly, these EVs were shown to transport the hHGSNAT-mRNA to bystander MPS IIIC cells, where the mRNA was translated into functional HGSNAT protein leading to the clearance of lysosomal GAG storage. Our data strongly support the therapeutic potential of rAAV-h*HGSNAT*^{EV} facilitated bystander effects via EV cargo for treating MPS IIIC.

2 | MATERIALS AND METHODS

2.1 | rAAV vectors

A rAAV vector plasmid, ptr-CMV-h*HGSNAT*^{EV}, was constructed to express hHGSNAT, in which a 25 nt EV-mRNA-zip code sequence (ACCCTGCCGCCTGGACTC CGCCTGT) (Bolukbasi et al., 2012) was incorporated into the 3′ untranslated region (3′UTR) of h*HGSNAT* cDNA. The rAAV-h*HGSNAT*^{EV} contains the human cytomegalovirus (CMV) immediate early enhancer-promoter and the bovine growth hormone Poly A signals. Another rAAV plasmid, ptr-CMV-h*HGSNAT*, without EV signal was constructed and used as control. These plasmids were used to produce rAAV-CMV-h*HGSNAT*^{EV} and rAAV-CMV-h*HGSNAT* viral vectors. These rAAV-h*HGSNAT* viral vector genomes contain only minimal elements required for transgene expression, including AAV2 inverted terminal repeats, h*HGSNAT*^{EV} or h*HGSNAT* cDNA, CMV promoter, and BGH Poly A signal.

rAAV2-h*HGSNAT*^{EV} and rAAV2-h*HGSNAT* viral vectors were manufactured by the UNC Vector Core, using triple transfection in HEK293 cells and purified using HPLC chromatography, and dialyzed into 1× PBS (pH 7.0) containing 5% sorbitol and 350 mM NaCl. The titter was determined by qPCR and confirmed by dot blot hybridization using HGSNAT coding sequence as probe and serially diluted linearized ptr-CMV-h*HGSNAT* plasmid as standard. Dot blot titter was used to guide the experiments.

2.2 | Cell cultures

Human MPS IIIC skin fibroblasts (GM05157), and normal human skin fibroblast cell line (GM00969), were obtained from Coriell Institute for Medical Research and used to test the rAAV vectors by transfection with the plasmids or infection with rAAV2 viral vectors. The cells were expanded at 37°C in Dulbecco's Modified Eagle Medium (DMEM) medium supplemented with 10% foetal bovine serum (FBS) and penicillin/streptomycin (pen/strep, 100 units/ml each). For experiments, cells were cultured in EV-free DMEM growth medium (DMEM medium supplemented with EV-free FBS and pen/strep). To obtain EV-free FBS, FBS was depleted of EVs by ultracentrifugation at 120,000 × *g* for 70 min followed by sterile filtration through a 0.22 μm filter.

2.3 | In vitro transduction

GM05157 cells were transduced by transfection with rAAV vector plasmids or rAAV2 viral vectors. For transfection, the GM05157 cells (70%–80% confluent) were transfected with the rAAV-h*HGSNAT* plasmid DNA (1 μg/10^6 cells) mixed with Polyethylenimine (PEI, 1 μg/2 μg DNA), following standard procedures. Six hours after the incubation, the media was replaced with EV-free DMEM growth media. For infection, GM05157 cells (70%–80% confluence) were infected with rAAV2-h*HGSNAT* viral vectors (3.5 × 10^{3}vg/cell) in EV-free DMEM growth media. The cells were cultured at 37°C for 48 h, and cells and medium were harvested and processed for analyses. Non-transduced GM05157 and GM00969 cells were used as controls.

2.4 | EV isolation

EV isolation was performed using ultracentrifugation as described previously (Ismail et al., 2013). Freshly collected media from transfected, or infected GM05157, and non-transduced controls cells, were centrifuged at 300 × *g* for 10 min at 4°C to remove residual cells. The supernatant was then centrifuged at 16,000 × *g* for 30 min at 4°C. The pellets were washed twice with cold phosphate-buffered saline (PBS, pH 7.4), followed by centrifugation at 16,000 × *g* for 30 min to remove contaminating proteins. The pelleted EVs were then either resuspended in PBS for analyses or in TRIzol for RNA extraction.

2.5 | In vitro EV-mRNA transfer

To assess EV-mRNA transfer, non-transduced GM05157 cells (70%–80% confluent) were incubated with isolated EVs or EV-containing media. The isolated EVs were added to 75% confluent GM05157 cells in EV-free DMEM growth medium. For conditioned media EV transfer, 75% confluent GM05157 cells were grown in cell-free media from AAV vector transfected or infected GM05157 cells after 48 h transduction, and non-transduced controls cells. The cells were then incubated at 37°C, and at 48 h of incubation, cells were processed for analyses for rHGSNAT activity, hHGSNAT mRNA, and GAG contents. Controls were GM05157 cells incubated in media from non-transduced GM05157 cells.

To obtain cell-free media, freshly harvested media from cultured cells were centrifuged at 300 × *g* for 10 min at 4°C, to remove residual cells.

2.6 | RNA isolation

Total cellular RNA and EV RNA were isolated from cells using TRIzol™ Reagent (Thermo Fisher Scientific), following the procedures provided by the manufacturer.

2.7 | Nanoparticle tracking analysis (NTA)

NTA were performed by nanomedicines characterization core facility at UNC, using Zetaview Quatt (ParticleMetrix, Germany). All samples were diluted to a concentration of 1–5 × 10^7 particles/mL in 20 μM filtered PBS (pH 7.4) and measured at scatter mode. Sensitivity was set at 80 and shutter at 100 for all measurements. Each sample was analysed at 11 positions. The Zetaview software was used to track the particles individually. Stokes-Einstein equation was used to calculate the hydrodynamic diameter (size) and concentration.

2.8 | Transmission electron microscopy (TEM)

TEM was performed by The Microscopy Services Laboratory at UNC-CH. Extracellular vesicle isolates were visualized by negative-stain TEM. A glow-discharged formvar/carbon-coated 400 mesh copper grids (Ted Pella, Inc., Redding, CA) was floated on a 20 μL droplet of the EV sample suspension for 10 min, and then transferred quickly to two drops of deionized water followed by a droplet of 2% aqueous uranyl acetate stain for 1 min. The grid was blotted with filter paper and air-dried, before being visualized using a JEOL JEM-1230 transmission electron microscope operating at 80 kV (JEOL USA INC., Peabody, MA). The images were taken using a Gatan Orius SC1000 CCD camera with Gatan Microscopy Suite version 3.10.1002.0 software (Gatan, Inc., Pleasanton, CA).

2.9 | Quantitative reverse transcription polymerase chain reaction (qRT-PCR)

Total RNA isolated from cells and EVs were assayed by qRT-PCR, following standard procedures. cDNA was synthesized from total RNA (1 μg) using Superscript III Reverse Transcriptase (Thermo Fisher Scientific). SYBR Green Mastermix (Thermo Fisher Scientific). Primers specific to hHGSNAT: forward: 5′-AGCTGAAGATGGATCAGG CT-3′; reverse: 5′-CCAGAACCTGAAACAAGCAG-3′ was used. mRNA expression was normalized to adenylate cyclase-associated protein 1 (CAP1): forward: 5′-ATTCCCTGGATTGTGA AATAGTC-3′; reverse: 5′-ATTAAAGTCACCGCCTTCTGTAG-3′.

2.10 | HGSNAT activity assay

Cell lysates were assayed for HGSNAT activity following previously published procedures (Voznyi et al., 1993). The assay measures 4-methylumbelliferone (Sigma), a fluorescent product formed by hydrolysis of the substrate 4-methylumbelliferyl-β-D-glucosamine (Moscerdam Substrates) supplemented with acetyl coenzyme A (Sigma). The HGSNAT activity is expressed as unit/mg protein. One unit is equal to 1 nmol 4-methylumbelliferone released/hr at 37°C.

2.11 | GAG content quantification

Cell samples were processed for total sulphated glycosaminoglycan (sGAG) contents using the glycosaminoglycan assay blyscan kit (Biocolor). The assays were performed following the procedures provided by the manufacturer. sGAG contents was expressed as $\mu g/5 \times 10^5$ cells.

3 | RESULTS

In this study, we developed two rAAV vectors expressing hHGSNAT. In one, rAAV-h*HGSNAT*^{EV}, we incorporated the 25 nt EV-mRNA packaging signal sequence at the 3′ end of the h*HGSNAT* cDNA (1908 bp, NM_152419.3) to generate EV-h*HGSNAT*-mRNA cargo. The second vector, rAAV-h*HGSNAT*, without the EV signal sequence was used as a control. The viral genomes of these vectors contain only minimal elements for transgene expression, including AAV2 ITRs, h*HGSNAT or* h*HGSNAT*^{EV} transgene, and the BGH poly A signal, driven by the CMV promoter. These vectors were tested in an in vitro model of human MPS IIIC.

Human MPS IIIC fibroblasts were transduced by the plasmid transfection or by infection with AAV2-h*HGSNAT* viral vectors. Freshly collected media samples from the transduced and control cells were processed to isolate EVs. Purified EVs were validated by testing multiple well-known EV markers and were analysed by NTA and TEM for further EV characterization and qRT-PCR for EV-hHGSNAT-mRNA packaging. Further, to determine the EV-mRNA transport, fresh media from MPS IIIC cells transfected with the AAV-h*HGSNAT* vector plasmids were incubated with non-treated MPS IIIC fibroblasts. Lysates of cells incubated with the conditioned media were analysed by qRT-PCR and HGSNAT activity assay to determine EV-mRNA transport, and GAG contents, to assess the cross-correction of lysosomal GAG storage facilitated by AAV-mediated EV-mRNA cargo. Figure S1 summarizes the overall study design.

3.1 | AAV-mediated rHGSNAT expression in human MPS IIIC cells

To assess the transduction efficiency and the therapeutic potential, we tested the vectors in human MPS IIIC skin fibroblasts by transfection with the vector plasmids and by infection with rAAV2 vectors. Healthy human skin fibroblasts and untreated MPS IIIC skin fibroblasts were used as controls. Forty-eight hours post-transfection or infection, cell lysates were assayed for HGSNAT activity and h*HGSNAT* mRNA by qRT-PCR, to determine the transgene expression levels. We detected 9-fold and 23-fold increases in HSGNAT activity in MPS IIIC cells transfected with AAV-h*HGSNAT* and AAV-h*HGSNAT*^{EV} vector plasmids, respectively, compared to healthy human cells (Figure 1a). qRT-PCR showed 37-fold and 107-fold increases in h*HGSNAT* mRNA levels in MPS IIIC cells transfected with AAV-h*HGSNAT* and AAV-*hHgsnat*^{EV} plasmids, respectively, compared to non-transduced MPS IIIC cells (Figure 1a). Similarly, supranormal levels of HGSNAT activity and significant levels of hHGSNAT-mRNA were detected in MPS IIIC cells infected with rAAV2-h*HGSNAT* and rAAV2-h*HGSNAT*^{EV} vectors (Figure 1b), though lower than expression in the transfected cells. Importantly, we observed no significant changes in cell viability between AAV-h*HGSNAT* and AAV-*hHgsnat*^{EV} transduction compared to non-treated controls (Figure S2). These results indicate that both of the AAV-h*HGSNAT* vectors mediated efficient hHGSNAT expression. Interestingly, inclusion of the EV-mRNA

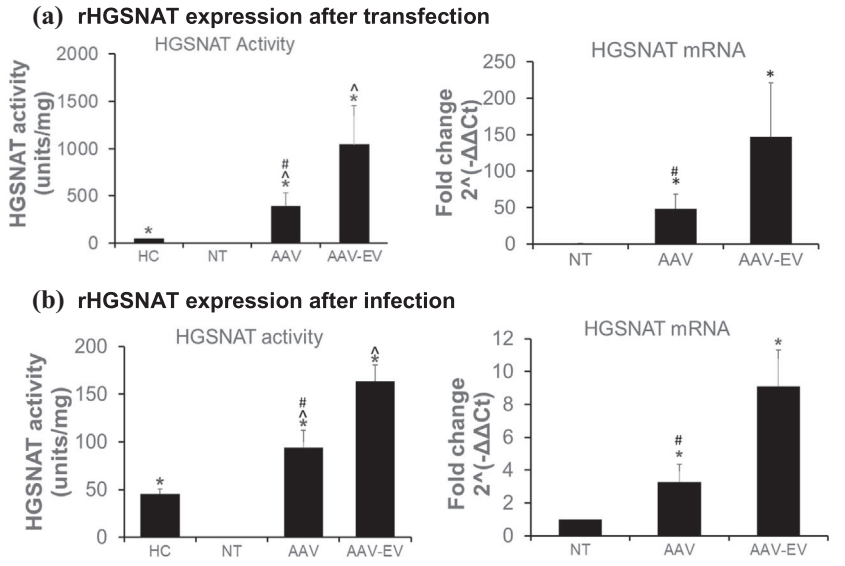

FIGURE 1 **AAV-mediated rHGSNAT expression in vitro in human MPS IIIC cells.** GM05157 cells were transfected in duplicates with the AAV-h*HGSNAT* vector plasmids (7 μg/plate) (a), or infected with rAAV2-h*HGSNAT* vectors (3.5×10^3vg/cell) (b). After 48 h incubation, cell lysates were assayed in duplicates for HGSNAT activity and for hHGSNAT mRNA by qRT-PCR. HGSNAT activity: units/mg protein, 1 unit = mmol 4MU released/hour. qRT-PCR data is expressed as fold of change 2^(−ΔΔCt) versus non-transduced cells (NT). HC: healthy human cells (GM00969); NT: non-treated MPS IIIC cells; AAV: MPS IIIC cells transfected or infected with AAV-HGSNAT vectors; AAV-EV: MPS IIIC cells transfected or infected with AAV-HGSNAT^{EV} vectors. *: $P < 0.05$ vs. NT; ^: $P < 0.05$ vs. HC; #: $P < 0.05$ vs. AAV-EV. Data were from 3 to 4 sets experiments each in duplicates, and each sample was assayed in duplicates.

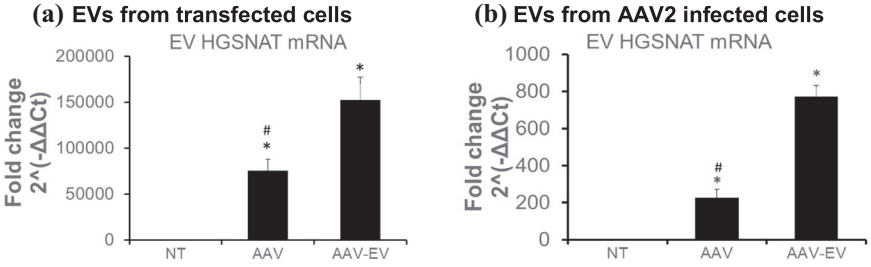

FIGURE 2 **AAV-mediated HGSNAT mRNA in EVs from human MPS IIIC cells.** 48 h post transfection or rAAV2 vector infection in GM05157 cells, media were processed to isolate EVs by ultracentrifugation. RNA extracted from EVs were assayed in duplicates by qRT-PCR for hHGSNAT mRNA, expressed as fold of change 2^(−ΔΔCt) versus NT samples. NT: EVs from non-treated MPS IIIC; AAV: EVs from MPS IIIC cells transfected or infected with AAV-h*HGSNAT* vectors; ZC: EVs from MPS IIIC cells transfected or infected with AAV-h*HGSNAT*^{EV} vectors. *: $P < 0.05$ vs. NT; #: $P < 0.05$ vs. AAV^{EV}. Data were from three sets experiments.

packaging signal sequence in the AAV-h*HGSNAT* vector significantly enhanced the HGSNAT expression at both the protein and mRNA levels (Figure 1). These data support the therapeutic potential of rAAV-h*HGSNAT* gene delivery for treating MPS IIIC.

3.2 | Incorporation of EV-mRNA packaging signal sequence in AAV-h*HGSNAT* vector promotes EV-HGSNAT-mRNA packaging

To assess the AAV-mediated EV-mRNA packaging, media from transduced MPS IIIC cells were processed to isolate EVs. RNAs extracted from the purified EVs were assayed by qRT-PCR for h*HGSNAT* mRNA to determine the targeted EV-mRNA packaging. Significant amounts of h*HGSNAT* mRNA were detected in EV-RNAs isolated from media from MPS IIIC cells transduced with AAV-h*HGSNAT*^{EV} or AAV-h*HGSNAT* vectors by transfection (Figure 2a) or infection (Figure 2b). As expected, EVs from AAV-h*HGSNAT*^{EV} infected cells contained much higher levels of HGSNAT-mRNA in EVs, vs. AAV-h*HGSNAT* vector (Figure 2). Further, a 190-fold higher mRNA level was detected in EVs from transfected cells (Figure 2a) compared to EVs from AAV-infected cells (Figure 2b). Of note, there was no detectable h*HGSNAT*-mRNAs in EVs isolated from media of non-transduced MPS IIIC cells (Figure 2). These data suggest that the ZC signal sequence increases EV packaging of HGSNAT-mRNA after rAAV treatment in MPS IIIC cells.

3.3 | AAV-h*HGSNAT* gene delivery diminished pathological EVs in MPS IIIC cells

To characterize the isolated EVs, nanoparticle-tracking analysis (NTA), and transmission electron microscopy (TEM) and EV-antibody array were performed to determine the EV quantity, size distribution, and morphology.

(a) EV NTA

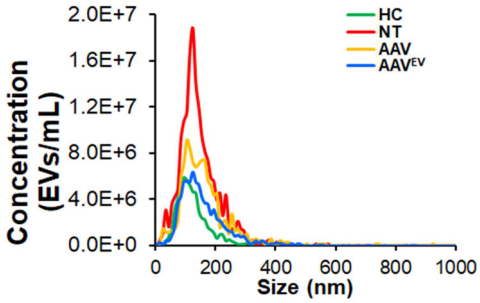

Cells	EV size (nm)	EV peak concentration (particles/ml)
HC	111.6	5.50E6
NT	125.9	1.27E7 ± 6.67E6
AAV (transfection)	144.8	8.45E6 ± 2.19E6
AAV^{EV} (transfection)	126.7	5.50E6 ± 4.24E5
AAV (infection)	135.1	5.90E6
AAV^{EV} (infection)	124.9	4.20E6

(b) EV TEM image

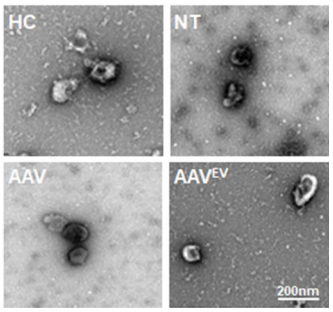

FIGURE 3 **Characterization of EVs and diminish of pathological EVs in MPS IIIC following AAV-h*HGSNAT* gene delivery**. MPS IIIC (GM05157) cells were transduce by plasmid transfection or rAAV2 infection. After 48 h incubation, media samples were processed to isolate EVs by ultracentrifugation. The isolated EVs were analysed using NanoSightNS500. HC: EVs from healthy control cells; NT: EVs from non-treated MPS IIIC cells; AAV: EVs from MPS IIIC cells transfected or infected with AAV-h*HGSNAT* vectors; AAV^{EV}: EVs from MPS IIIC cells transfected or infected with AAV-h*HGSNAT*^{EV} vectors. Data were from three sets of plasmid transfections and two sets of AAV2 infections.

The NTA showed that the EVs were consistent in sizes ranging from 50 to 150 nm among different experimental groups, with the majority (>98%) sized 111.6–144.8 nm (Figure 3a). Consistent with the NTA results, the TEM analysis revealed a heterogenous population of EVs in size and appearance, regardless of experiment conditions (Figure 3b). Interestingly, we observed approximately 2-fold more EVs released from non-treated MPS IIIC cells (1.27E7/10^6 cells) than from healthy cells (5.5E6/10^6 cells) (Figure 3a), though all of the EV samples were normalized to the number of cells. Importantly, the quantity of EVs isolated from treated MPS IIIC cells by transfection or infection were at levels comparable to normal cells (Figure 3a). Notably, increases in EV excretion have been linked to various diseases, suggesting that the increase in EV quantity from the MPS IIIC cells is due to the disease pathology. The EV reduction following AAV-h*HGSNAT* transduction suggests the correction of the pathophysiological condition, supporting the therapeutic potential of AAV-h*HGSNAT* gene therapy.

EV samples were assayed with an EV-antibody array for eight known exosome markers (CD63, CD81, ALIX, FLOT1, ICAM1, EpCAM, ANXA5 and TSG101), as well as a cellular marker (GM130) for potential cellular contamination during EV isolation. EVs from MPS IIIC fibroblasts (treated and non-treated) were positive for CD63, FLOT1, ICAM, EpCAM, ANXA5, TSG101, and ALIX. Interestingly, EVs from healthy fibroblasts were positive for CD63, FLOT1, ICAM and ALIX at a lower intensity (Figure S3). Notably, for both healthy and MPS IIIC EVs, ALIX, a known marker for exosome formation, was the most significant marker observed. Further, all purified EVs stained negative for GM130, indicating that these EVs samples were free of cellular contamination.

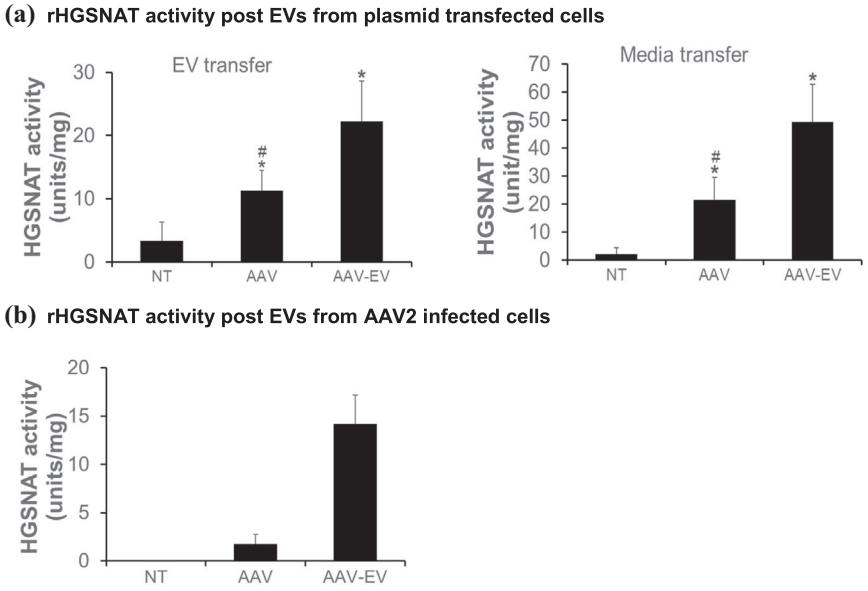

FIGURE 4 **Expression of rHGSNAT in recipient MPS IIIC cells following EV-mRNA transfer**. MPS IIIC (GM05157) cells were transduce by plasmid transfection or rAAV2 infection. After 48 h incubation, media samples were processed to isolate EVs by ultracentrifugation. Non-treated GM05157 cells were incubated with isolated EVs for 48 h and cell lysates were then assayed in duplicate for HGSNAT activity. HGSNAT activity is expressed as units/mg protein, 1 unit = nmol 4MU released/hour. NT: non-treated MPS IIIC cells; AAV: MPS IIIC cells incubated with EVs isolated from MPS IIIC cells transfected or infected with AAV-h*HGSNAT* vectors; AAV^{EV}: MPS IIIC cells incubated with EVs isolated from MPS IIIC cells transfected or infected with AAV-h*HGSNAT*^{EV} vectors. *: $P < 0.05$ vs. NT; $^{\#}$: $P < 0.05$ vs. AAV-EV. (Data were from two to three sets experiments each in duplicates.).

3.4 | EV-mRNA transfer led to the expression of functional HGSNAT protein in bystander MPS IIIC cells

To assess EV-mRNA transport, non-treated MPS IIIC cells were incubated with isolated EVs or conditioned media from MPS IIIC cells that were transduced with the AAV-h*HGSNAT*^{EV} or AAV-h*HGSNAT* vectors, either by plasmid transfection or AAV2 infection. Forty-eight hours post EV or media incubation, the recipient MPS IIIC cell lysates were assayed for HGSNAT enzyme activity and mRNA levels.

HGSNAT activity was detected in each of the cell lysates of MPS IIIC cells incubated with EVs or conditioned media from cells that were transduced with AAV-h*HGANAT*^{EV} (Figure 4a) or AAV-h*HGANAT* (Figure 4b) vectors. However, incubation with EVs or media from cells transfected with AAV-h*HGSNAT*^{EV} led to significantly higher HGSNAT activity (Figure 4) in the recipient MPS IIIC cells compared to EVs from cells treated with AAV-h*HGSNAT* control vector. In addition, low levels of hHGSNAT-mRNA were detected in recipient MPS IIIC cells incubated with isolated EVs or media from MPS IIIC cells transfected with AAV-h*HGSNAT*^{EV} vectors (Figure S4). These results indicate that HGSNAT-mRNA was transported to the recipient cells by rAAV-mediated EVs and translated into enzymatically functional HGSNAT protein in the recipient cells. Further, incorporation of the EV-mRNA packaging signal into the rAAV-*hHGSNAT* vector promotes loading of EV-HGSNAT-mRNA cargo.

3.5 | Clearance of GAG storage in MPS IIIC cells following transduction and AAV-mediated EV mRNA transfer

To further assess the function of rAAV-mediated rHGSNAT expression, lysates from transfected MPS IIIC cells, or cells that were incubated with conditioned media from transfected MPS IIIC cells, were assayed for GAG content. The results showed the reduction of GAG contents to normal levels in MPS IIIC fibroblasts transfected with both AAV-h*HGSNAT*^{EV} and AAV-h*HGSNAT* vector constructs (Figure 5a). Interestingly, incubation with media from cells transduced with AAV-h*HGSNAT*^{EV} resulted in the decrease of GAG contents to normal levels in recipient MPS IIIC cells (Figure 5b), while partial GAG reduction was observed in MPS IIIC cells incubated with media from MPS IIIC cells transduced with control AAV-h*HGSNAT* plasmid (Figure 5b). These data support the functionality of AAV-mediated rHGSNAT leading to the clearance of GAG storage. Specifically, mRNA transfer by the AAV-mediated EV cargo led to the translation of hHGSNAT-mRNA to functional rHGSNAT protein in MPS IIIC cells.

4 | DISCUSSION

In this study, we targeted the critical unmet need for MPS IIIC therapy by developing a novel rAAV gene replacement vector, rAAV-h*HGSNAT*^{EV}, in an attempt to facilitate bystander effects and cross-correction via targeted EV-mRNA cargo, given that the missing enzyme (HGSNAT) in MPS IIIC is a non-secretory trans-lysosomal membrane protein. Our data showed that incorporating the 25 nt EV-mRNA packaging signal to rAAV-h*HGSNAT* vector within the 3′UTR of h*HGSNAT* cDNA enhanced

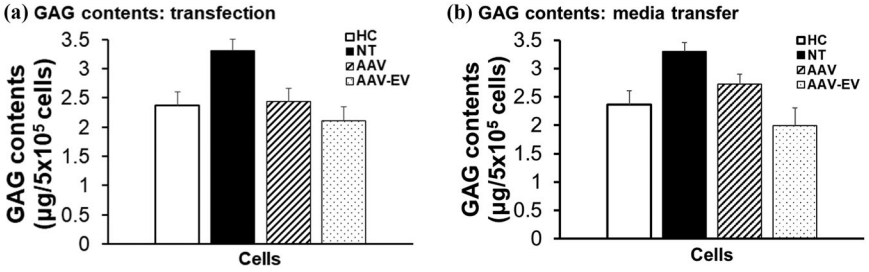

FIGURE 5 **AAV-mediated clearance of GAG storage in human MPS IIIC cells**. GM05157 cells were transfected in duplicates with AAV-h*HGSNAT or AAV*V-h*HGSNAT*^{zc} plasmids, and cells and media were collected 48 h later. The media collected from transfected cells were added to non-treated GM05157 cells and incubated for 48 h. Transfected cell lysates (a) and lysates of cells incubated with media from transfected cells (b) were assayed in duplicates for GAG contents (μg/5e10 cells). HC: healthy human fibroblasts; NT: Non-treated GM05157 cells; AAV: GM05157 transfected with AAV-h*HGSNAT* plasmid (a) or incubated with media of cells transfected with AAV-h*HGSNAT* (b); AAV-EV: GM05157 transfected with AAV-hHGSNAT^{EV} plasmid (a) or incubated with media of AAV-h*HGSNAT*^{EV} transfected cells (b).

transgene expression at both the protein and mRNA levels in MPS IIIC cells. While the mechanisms remain unclear regarding the enhanced transgene expression levels, mRNA 3′UTRs are known to regulate mRNA processes, including mRNA stability, localization and translation, and protein post-translational modification. (Mayr, 2019) Therefore, including the EV-mRNA packaging signal at the 3′UTR of the transgene in an rAAV vector may mediate not only the transport of the transgene mRNA to EVs, but also enhanced transgene expression due to targeted mRNA regulation. Further, the rHGSNAT expression mediated by rAAV-h*HGSNAT*^{EV} or rAAV-h*HGSNAT* vector was sufficient to clear the accumulation of GAG contents in MPS IIIC cells at effective doses.

As hypothesized, this study also demonstrated that incorporating the EV-mRNA packaging signal into the rAAV vector construct indeed enhanced the release of hHGSNAT-mRNA-containing EVs by transduced MPS IIIC cells. Unsurprisingly, we observed significantly higher mRNA levels in EVs from MPS IIIC cells following plasmid transfection compared to AAV2 infection, because transfection allows more vector plasmid DNA to enter the cells via electrical force than rAAV viral vectors that requires receptor-mediated binding, this generally results in high vector copies per cell and therefore greater EV-mRNA packaging. Notably, in this study, the sizes of EVs were largely heterogeneous, with the majority at 111.6–144.8 nm, regardless of the disease status or experimental conditions. It is likely that these EVs are mostly exosomes and small microvesicles, although we did not perform assays to distinguish one from the other. Interestingly, transduction with rAAV-h*HGSNAT* vector without the EV-mRNA packaging signal also mediated the release of EVs containing hHGSNAT-mRNA, but at significantly lower levels. This is not surprising, since overexpression of a particular mRNA can induce passive loading of that mRNA in EVs (O'Brien et al., 2020) and numerous studies showed that changes in biophysiological conditions could trigger EV level changes, and changes in EV levels have been linked to physiological and pathophysiological conditions, such as autoimmune diseases including multiple sclerosis (MS) and cancer, in which increases in EV levels have been reported (Logozzi et al., 2009; Robbins & Morelli, 2014; Sáenz-Cuesta et al., 2014). It is therefore possible that the transduction of MPS IIIC cells with rAAV-h*HGSNAT* vector may be sufficient to induce hHGSNAT-mRNA-EVs.

Notably, we demonstrated here not only the AAV-mediated targeted EV-mRNA packaging, but also the successful transport of hHGSNAT-mRNA by the AAV-mediated EVs into the non-transduced MPS IIIC cells, where the hHGSNAT-mRNA released from the EVs was translated into enzymatically functional rHGSNAT protein, leading to the restoration of HGSNAT activity in the recipient MPS IIIC cells. Importantly, the AAV-mediated EV-hHGSNAT-mRNA transfer also resulted in the clearance of the GAG contents accumulation in the recipient MPS IIIC cells. The HGSNAT gene product is a lysosomal enzyme and an exclusively trans-lysosomal-membrane protein. It is not soluble in the aqueous cytosolic or extracellular environments. Therefore, our data further demonstrates that rHGSNAT translated from the EV-HGSNAT-mRNA transfer was correctly processed via appropriate post-translational modification to form the fully functional trans-lysosomal membrane HGSNAT protein, because the observed cross correction of lysosomal GAG storage could only be achieved in the presence of the trans-lysosomal membrane HGSNAT protein. These observations strongly support the therapeutic potential of incorporating the EV-mRNA packaging signal in rAAV gene replacement vectors for treating MPS IIIC, and possibly other neurogenetic diseases involving non-secreted proteins or transcriptional factors, since this approach may allow greater therapeutic benefits without having to transduce every cell.

Further, in this study, for the first time, we observed the release of 2-fold more EVs by non-treated MPS IIIC cells than normal healthy control cells, suggesting that there is a significant increase in EVs in MPS IIIC. While detailed mechanisms are unclear, numerous studies have reported EV increases in different disease conditions (Logozzi et al., 2009; Robbins & Morelli, 2014; Sáenz-Cuesta et al., 2014). This is supported by our findings that while EVs from both MPS IIIC and healthy cells were positive for 4 exosome markers, CD63, FLOT1, ICAM and ALIX, the levels of these markers were significantly lower in healthy cells. Interestingly, only EVs from MPS IIIC (but not healthy cells) were also positive for EpCAM, ANXA5 and TSG101. We therefore

believe that the increase in the levels and markers of EVs released by MPS IIIC cells is likely pathological changes triggered directly or indirectly by the primary pathology of MPS IIIC, the lysosomal GAG accumulation.

Importantly, transduction of MPS IIIC cells with rAAV-h*HGSNAT*^{EV} or AAV-h*HGSNAT* vector resulted in the reduction of EVs to normal levels, though did not have detectable impacts on the EV markers. These data demonstrate that AAV-mediated restoration of HGSNAT activity in MPS IIIC cells diminished the lysosomal storage pathology, leading to the correction of the pathological levels of EVs, thus supporting the therapeutic potential of AAV-h*HGSNAT* gene therapy. However, it is unclear why the gene therapy treatment did not correct the EV marker changes in MPS IIIC cells.

In summary, in this study, the incorporation of an EV-mRNA packaging zip code sequence in rAAV-h*HGSNAT*^{EV} gene therapy vector did not only mediate effective transgene expression, but also enhanced the targeted EV-hHGSNAT-mRNA packaging. Importantly, the EVs can transport the hHGSNAT-mRNA into MPS IIIC cells, where it can be translated to functional HGSNAT protein, leading to the cross-correction of lysosomal storage pathology in the bystander MPS IIIC cells. These results strongly support the therapeutic potential of this novel rAAV gene therapy approach for the treatment of MPS IIIC. We believe that this approach is broadly applicable for targeting diseases involving non-secreted proteins or transcriptional factors, specifically addressing the challenge of the potential safety concerns due to high vector dose requirements.

AUTHOR CONTRIBUTIONS

Tierra Amber Bobo: Conceptualization; Data curation; Formal analysis; Investigation; Methodology; Supervision; Validation; Writing—original draft; Writing—review and editing. Michael Robinson: Formal analysis; investigation. Christopher Tofade: Formal analysis; investigation. Peter Grant Nichols: Investigation. Stephen Mitchell Vorobiov: Investigation. Haiyan Fu: Conceptualization; formal analysis; funding acquisition; investigation; methodology; supervision; validation; writing—original draft; writing—review and editing.

ACKNOWLEDGEMENTS

We thank the Nanomedicine Characterization Core Facility at UNC Eshelman School of Pharmacy for providing NTA analyses. We also thank Kristen K. White of The Microscopy Services Laboratory at UNC for assisting us in TEM analysis. We appreciate Dr. Douglas M. McCarty's constructive comments and editing assistance. TB was supported by a Gene Therapy Fellowship from North Carolina Biotechnology Center (NCBC 2020-GTF-6903) and the Muenzer MPS Research & Treatment Center. This study was also supported by a research grant from the NIH (R21NS118165). The UNC Microscopy Services Laboratory, is supported in part by an NIH grant (P30 CA016086).

CONFLICT OF INTEREST STATEMENT

This work has led to an IP disclosure (WO 2023/019189 A1), for which NeuroGT, Inc. holds exclusive license. HF is the founder and President of NeuroGT, Inc.

ORCID

Tierra A. Bobo https://orcid.org/0000-0002-1624-5067

REFERENCES

Andrade, F., Aldámiz-Echevarría, L., Llarena, M., & Couce, M. L. (2015). Sanfilippo syndrome: Overall review. *Pediatrics international : official journal of the Japan Pediatric Society*, *57*(3), 331–338.

Bailey, R. M., Armao, D., Nagabhushan Kalburgi, S., & Gray, S. J. (2018). Development of intrathecal AAV9 gene therapy for giant axonal neuropathy. *Molecular Therapy. Methods & Clinical Development*, *9*, 160–171. https://doi.org/10.1016/j.omtm.2018.02.005

Barile, L., & Vassalli, G. (2017). Exosomes: Therapy delivery tools and biomarkers of diseases. *Pharmacology & Therapeutics*, *174*, 63–78. https://doi.org/10.1016/j.pharmthera.2017.02.020

Belting, M., & Wittrup, A. (2008). Nanotubes, exosomes, and nucleic acid-binding peptides provide novel mechanisms of intercellular communication in eukaryotic cells: Implications in health and disease. *The Journal of Cell Biology*, *183*(7), 1187–1191. https://doi.org/10.1083/jcb.200810038

Berns, K. I., & Giraud, C. (1996). Biology of adeno-associated virus. *Current Topics in Microbiology and Immunology*, *218*, 1–23. https://doi.org/10.1007/978-3-642-80207-2_1

Bevan, A. K., Duque, S., Foust, K. D., Morales, P. R., Braun, L., Schmelzer, L., Chan, C. M., McCrate, M., Chicoine, L. G., Coley, B. D., Porensky, P. N., Kolb, S. J., Mendell, J. R., Burghes, A. H., & Kaspar, B. K. (2011). Systemic gene delivery in large species for targeting spinal cord, brain, and peripheral tissues for pediatric disorders. *Molecular Therapy: The Journal of the American Society of Gene Therapy*, *19*(11), 1971–1980. https://doi.org/10.1038/mt.2011.157

Bobo, T. A., Samowitz, P. N., Robinson, M. I., & Fu, H. (2020). Targeting the root cause of mucopolysaccharidosis IIIA with a new scAAV9 gene replacement vector. *Molecular Therapy. Methods & Clinical Development*, *19*, 474–485. https://doi.org/10.1016/j.omtm.2020.10.014

Bolukbasi, M. F., Mizrak, A., Ozdener, G. B., Madlener, S., Ströbel, T., Erkan, E. P., Fan, J. B., Breakefield, X. O., & Saydam, O. (2012). miR-1289 and "Zipcode"-like sequence enrich mRNAs in microvesicles. *Molecular Therapy. Nucleic Acids*, *1*(2), e10. https://doi.org/10.1038/mtna.2011.2

Bolukbasi, M. F., Mizrak, A., Ozdener, G. B., Madlener, S., Ströbel, T., Erkan, E. P., Fan, J. B., Breakefield, X. O., & Saydam, O. (2012). miR-1289 and "Zipcode"-like sequence enrich mRNAs in microvesicles. *Molecular Therapy. Nucleic Acids*, *1*(2), e10. https://doi.org/10.1038/mtna.2011.2

Cain, J. T., Likhite, S., White, K. A., Timm, D. J., Davis, S. S., Johnson, T. B., Dennys-Rivers, C. N., Rinaldi, F., Motti, D., Corcoran, S., Morales, P., Pierson, C., Hughes, S. M., Lee, S. Y., Kaspar, B. K., Meyer, K., & Weimer, J. M. (2019). Gene therapy corrects brain and behavioral pathologies in CLN6-batten disease. *Molecular Therapy: The Journal of the American Society of Gene Therapy*, *27*(10), 1836–1847. https://doi.org/10.1016/j.ymthe.2019.06.015

Colombo, M., Raposo, G., & Théry, C. (2014). Biogenesis, secretion, and intercellular interactions of exosomes and other extracellular vesicles. *Annual Review of Cell and Developmental Biology*, *30*, 255–289. https://doi.org/10.1146/annurev-cellbio-101512-122326

de Jong, O. G., Kooijmans, S. A. A., Murphy, D. E., Jiang, L., Evers, M. J. W., Sluijter, J. P. G., Vader, P., & Schiffelers, R. M. (2019). Drug delivery with extracellular vesicles: From imagination to innovation. *Accounts of Chemical Research*, *52*(7), 1761–1770. https://doi.org/10.1021/acs.accounts.9b00109

Duque, S., Joussemet, B., Riviere, C., Marais, T., Dubreil, L., Douar, A. M., Fyfe, J., Moullier, P., Colle, M. A., & Barkats, M. (2009). Intravenous administration of self-complementary AAV9 enables transgene delivery to adult motor neurons. *Molecular Therapy: The Journal of The American Society of Gene Therapy*, *17*(7), 1187–1196. https://doi.org/10.1038/mt.2009.71

Duque, S. I., Arnold, W. D., Odermatt, P., Li, X., Porensky, P. N., Schmelzer, L., Meyer, K., Kolb, S. J., Schümperli, D., Kaspar, B. K., & Burghes, A. H. (2015). A large animal model of spinal muscular atrophy and correction of phenotype. *Annals of Neurology*, *77*(3), 399–414. https://doi.org/10.1002/ana.24332

Fatima, F., & Nawaz, M. (2017). Long distance metabolic regulation through adipose-derived circulating exosomal miRNAs: A trail for RNA-based therapies? *Frontiers in Physiology*, *8*, 545. https://doi.org/10.3389/fphys.2017.00545

Foust, K. D., Nurre, E., Montgomery, C. L., Hernandez, A., Chan, C. M., & Kaspar, B. K. (2009). Intravascular AAV9 preferentially targets neonatal neurons and adult astrocytes. *Nature Biotechnology*, *27*(1), 59–65. https://doi.org/10.1038/nbt.1515

Foust, K. D., Wang, X., McGovern, V. L., Braun, L., Bevan, A. K., Haidet, A. M., Le, T. T., Morales, P. R., Rich, M. M., Burghes, A. H., & Kaspar, B. K. (2010). Rescue of the spinal muscular atrophy phenotype in a mouse model by early postnatal delivery of SMN. *Nature Biotechnology*, *28*(3), 271–274. https://doi.org/10.1038/nbt.1610

Fu, H., Cataldi, M. P., Ware, T. A., Zaraspe, K., Meadows, A. S., Murrey, D. A., & McCarty, D. M. (2016). Functional correction of neurological and somatic disorders at later stages of disease in MPS IIIA mice by systemic scAAV9-hSGSH gene delivery. *Molecular Therapy. Methods & Clinical Development*, *3*, 16036. https://doi.org/10.1038/mtm.2016.36

Fu, H., Dirosario, J., Killedar, S., Zaraspe, K., & McCarty, D. M. (2011). Correction of neurological disease of mucopolysaccharidosis IIIB in adult mice by rAAV9 trans-blood-brain barrier gene delivery. *Molecular Therapy: The Journal of the American Society of Gene Therapy*, *19*(6), 1025–1033.

Fu, H., Zaraspe, K., Murakami, N., Meadows, A. S., Pineda, R. J., McCarty, D. M., & Muenzer, J. (2018). Targeting root cause by systemic scAAV9-h*IDS* gene delivery: Functional correction and reversal of severe MPS II in mice. *Molecular Therapy. Methods & Clinical Development*, *10*, 327–340. https://doi.org/10.1016/j.omtm.2018.07.005

Gassama, Y., & Favereaux, A. (2021). Emerging roles of extracellular vesicles in the central nervous system: Physiology, pathology, and therapeutic perspectives. *Frontiers in Cellular Neuroscience*, *15*, 626043. https://doi.org/10.3389/fncel.2021.626043

Gross, A. L., Gray-Edwards, H. L., Bebout, C. N., Ta, N. L., Nielsen, K., Brunson, B. L., Lopez Mercado, K. R., Osterhoudt, D. E., Batista, A. R., Maitland, S., Seyfried, T. N., Sena-Esteves, M., & Martin, D. R. (2022). Intravenous delivery of adeno-associated viral gene therapy in feline GM1 gangliosidosis. *Brain: A Journal of Neurology*, *145*(2), 655–669. https://doi.org/10.1093/brain/awab309

Gurda, B. L., De Guilhem De Lataillade, A., Bell, P., Zhu, Y., Yu, H., Wang, P., Bagel, J., Vite, C. H., Sikora, T., Hinderer, C., Calcedo, R., Yox, A. D., Steet, R. A., Ruane, T., O'Donnell, P., Gao, G., Wilson, J. M., Casal, M., Ponder, K. P., & Haskins, M. E. (2016). Evaluation of AAV-mediated gene therapy for central nervous system disease in canine mucopolysaccharidosis VII. *Molecular Therapy: The Journal of the American Society of Gene Therapy*, *24*(2), 206–216. https://doi.org/10.1038/mt.2015.189

Haurigot, V., Marcó, S., Ribera, A., Garcia, M., Ruzo, A., Villacampa, P., Ayuso, E., Añor, S., Andaluz, A., Pineda, M., García-Fructuoso, G., Molas, M., Maggioni, L., Muñoz, S., Motas, S., Ruberte, J., Mingozzi, F., Pumarola, M., & Bosch, F. (2013). Whole body correction of mucopolysaccharidosis IIIA by intracerebrospinal fluid gene therapy. *The Journal of Clinical Investigation*, *123*(8), 3254–3271. https://doi.org/10.1172/JCI66778

Hedlund, M., Nagaeva, O., Kargl, D., Baranov, V., & Mincheva-Nilsson, L. (2011). Thermal- and oxidative stress causes enhanced release of NKG2D ligand-bearing immunosuppressive exosomes in leukemia/lymphoma T and B cells. *PLoS ONE*, *6*(2), e16899. https://doi.org/10.1371/journal.pone.0016899

Hinderer, C., Bell, P., Gurda, B. L., Wang, Q., Louboutin, J. P., Zhu, Y., Bagel, J., O'Donnell, P., Sikora, T., Ruane, T., Wang, P., Haskins, M. E., & Wilson, J. M. (2014). Intrathecal gene therapy corrects CNS pathology in a feline model of mucopolysaccharidosis I. *Molecular Therapy: The Journal of the American Society of Gene Therapy*, *22*(12), 2018–2027. https://doi.org/10.1038/mt.2014.135

Hinderer, C., Katz, N., Louboutin, J. P., Bell, P., Yu, H., Nayal, M., Kozarsky, K., O'Brien, W. T., Goode, T., & Wilson, J. M. (2016). Delivery of an adeno-associated virus vector into cerebrospinal fluid attenuates central nervous system disease in mucopolysaccharidosis type II mice. *Human gene Therapy*, *27*(11), 906–915. https://doi.org/10.1089/hum.2016.101

Hudry, E., & Vandenberghe, L. H. (2019). Therapeutic AAV gene transfer to the nervous system: A clinical reality. *Neuron*, *101*(5), 839–862. https://doi.org/10.1016/j.neuron.2019.02.017

Ismail, N., Wang, Y., Dakhlallah, D., Moldovan, L., Agarwal, K., Batte, K., Shah, P., Wisler, J., Eubank, T. D., Tridandapani, S., Paulaitis, M. E., Piper, M. G., & Marsh, C. B. (2013). Macrophage microvesicles induce macrophage differentiation and miR-223 transfer. *Blood*, *121*(6), 984–995. https://doi.org/10.1182/blood-2011-08-374793

Kossinova, O. A., Gopanenko, A. V., Tamkovich, S. N., Krasheninina, O. A., Tupikin, A. E., Kiseleva, E., Yanshina, D. D., Malygin, A. A., Ven'yaminova, A. G., Kabilov, M. R., & Karpova, G. G. (2017). Cytosolic YB-1 and NSUN2 are the only proteins recognizing specific motifs present in mRNAs enriched in exosomes. *Biochimica et Biophysica Acta. Proteins and Proteomics*, *1865*(6), 664–673. https://doi.org/10.1016/j.bbapap.2017.03.010

Lässer, C., Shelke, G. V., Yeri, A., Kim, D. K., Crescitelli, R., Raimondo, S., Sjöstrand, M., Gho, Y. S., Van Keuren Jensen, K., & Lötvall, J. (2017). Two distinct extracellular RNA signatures released by a single cell type identified by microarray and next-generation sequencing. *RNA Biology*, *14*(1), 58–72. https://doi.org/10.1080/15476286.2016.1249092

Lavery, C., Hendriksz, C. J., & Jones, S. A. (2017). Mortality in patients with Sanfilippo syndrome. *Orphanet Journal of Rare Diseases*, *12*(1), 168.

Lee, N. C., Muramatsu, S., Chien, Y. H., Liu, W. S., Wang, W. H., Cheng, C. H., Hu, M. K., Chen, P. W., Tzen, K. Y., Byrne, B. J., & Hwu, W. L. (2015). Benefits of neuronal preferential systemic gene therapy for neurotransmitter deficiency. *Molecular Therapy: The Journal of the American Society of Gene Therapy*, *23*(10), 1572–1581. https://doi.org/10.1038/mt.2015.122

Li, J., Liu, K., Liu, Y., Xu, Y., Zhang, F., Yang, H., Liu, J., Pan, T., Chen, J., Wu, M., Zhou, X., & Yuan, Z. (2013). Exosomes mediate the cell-to-cell transmission of IFN-α-induced antiviral activity. *Nature Immunology*, *14*(8), 793–803. https://doi.org/10.1038/ni.2647

Li, X., Corbett, A. L., Taatizadeh, E., Tasnim, N., Little, J. P., Garnis, C., Daugaard, M., Guns, E., Hoorfar, M., & Li, I. T. S. (2019). Challenges and opportunities in exosome research – Perspectives from biology, engineering, and cancer therapy. *APL Bioengineering*, *3*(1), 011503. https://doi.org/10.1063/1.5087122

Logozzi, M., De Milito, A., Lugini, L., Borghi, M., Calabrò, L., Spada, M., Perdicchio, M., Marino, M. L., Federici, C., Iessi, E., Brambilla, D., Venturi, G., Lozupone, F., Santinami, M., Huber, V., Maio, M., Rivoltini, L., & Fais, S. (2009). High levels of exosomes expressing CD63 and caveolin-1 in plasma of melanoma patients. *PLoS ONE*, *4*(4), e5219. https://doi.org/10.1371/journal.pone.0005219

Mayr, C. (2019). What are 3′ UTRs doing? *Cold Spring Harbor Perspectives in Biology*, *11*(10), a034728. https://doi.org/10.1101/cshperspect.a034728

Meldolesi, J. (2019). Extracellular vesicles, news about their role in immune cells: Physiology, pathology and diseases. *Clinical and Experimental Immunology*, *196*(3), 318–327. https://doi.org/10.1111/cei.13274

Meldolesi, J. (2021). Extracellular vesicles (exosomes and ectosomes) play key roles in the pathology of brain diseases. *Molecular Biomedicine*, *2*(1), 18. https://doi.org/10.1186/s43556-021-00040-5

Mendell, J. R., Al-Zaidy, S., Shell, R., Arnold, W. D., Rodino-Klapac, L. R., Prior, T. W., Lowes, L., Alfano, L., Berry, K., Church, K., Kissel, J. T., Nagendran, S., L'Italien, J., Sproule, D. M., Wells, C., Cardenas, J. A., Heitzer, M. D., Kaspar, A., Corcoran, S., … Kaspar, B. K. (2017). Single-dose gene-replacement therapy for spinal muscular atrophy. *The New England Journal of Medicine*, *377*(18), 1713–1722. https://doi.org/10.1056/NEJMoa1706198

Meyer, K., Ferraiuolo, L., Schmelzer, L., Braun, L., McGovern, V., Likhite, S., Michels, O., Govoni, A., Fitzgerald, J., Morales, P., Foust, K. D., Mendell, J. R., Burghes, A. H., & Kaspar, B. K. (2015). Improving single injection CSF delivery of AAV9-mediated gene therapy for SMA: A dose-response study in mice and nonhuman primates. *Molecular Therapy: The Journal of the American Society of Gene Therapy*, *23*(3), 477–487. https://doi.org/10.1038/mt.2014.210

Mittelbrunn, M., & Sánchez-Madrid, F. (2012). Intercellular communication: Diverse structures for exchange of genetic information. *Nature Reviews. Molecular Cell Biology*, *13*(5), 328–335. https://doi.org/10.1038/nrm3335

Mizrak, A., Bolukbasi, M. F., Ozdener, G. B., Brenner, G. J., Madlener, S., Erkan, E. P., Ströbel, T., Breakefield, X. O., & Saydam, O. (2013). Genetically engineered microvesicles carrying suicide mRNA/protein inhibit schwannoma tumor growth. *Molecular Therapy: The Journal of the American Society of Gene Therapy*, *21*(1), 101–108. https://doi.org/10.1038/mt.2012.161

Montecalvo, A., Larregina, A. T., Shufesky, W. J., Stolz, D. B., Sullivan, M. L., Karlsson, J. M., Baty, C. J., Gibson, G. A., Erdos, G., Wang, Z., Milosevic, J., Tkacheva, O. A., Divito, S. J., Jordan, R., Lyons-Weiler, J., Watkins, S. C., & Morelli, A. E. (2012). Mechanism of transfer of functional microRNAs between mouse dendritic cells via exosomes. *Blood*, *119*(3), 756–766. https://doi.org/10.1182/blood-2011-02-338004

Mussche, S., Devreese, B., Nagabhushan Kalburgi, S., Bachaboina, L., Fox, J. C., Shih, H. J., Van Coster, R., Samulski, R. J., & Gray, S. J. (2013). Restoration of cytoskeleton homeostasis after gigaxonin gene transfer for giant axonal neuropathy. *Human Gene Therapy*, *24*(2), 209–219. https://doi.org/10.1089/hum.2012.107

Neufeld, E. F., & Cantz, M. J. (1971). Corrective factors for inborn errors of mucopolysaccharide metabolism. *Annals of the New York Academy of Sciences*, *179*, 580–587. https://doi.org/10.1111/j.1749-6632.1971.tb46934.x

O'Brien, K., Breyne, K., Ughetto, S., Laurent, L. C., & Breakefield, X. O. (2020). RNA delivery by extracellular vesicles in mammalian cells and its applications. *Nature Reviews. Molecular Cell Biology*, *21*(10), 585–606. https://doi.org/10.1038/s41580-020-0251-y

Rapoport, S. I. (2000). Osmotic opening of the blood-brain barrier: Principles, mechanism, and therapeutic applications. *Cellular and Molecular Neurobiology*, *20*(2), 217–230. https://doi.org/10.1023/a:1007049806660

Ribera, A., Haurigot, V., Garcia, M., Marcó, S., Motas, S., Villacampa, P., Maggioni, L., León, X., Molas, M., Sánchez, V., Muñoz, S., Leborgne, C., Moll, X., Pumarola, M., Mingozzi, F., Ruberte, J., Añor, S., & Bosch, F. (2015). Biochemical, histological and functional correction of mucopolysaccharidosis type IIIB by intra-cerebrospinal fluid gene therapy. *Human Molecular Genetics*, *24*(7), 2078–2095. https://doi.org/10.1093/hmg/ddu727

Robbins, P. D., & Morelli, A. E. (2014). Regulation of immune responses by extracellular vesicles. *Nature Reviews. Immunology*, *14*(3), 195–208. https://doi.org/10.1038/nri3622

Ruzo, A., Marcó, S., García, M., Villacampa, P., Ribera, A., Ayuso, E., Maggioni, L., Mingozzi, F., Haurigot, V., & Bosch, F. (2012). Correction of pathological accumulation of glycosaminoglycans in central nervous system and peripheral tissues of MPSIIIA mice through systemic AAV9 gene transfer. *Human Gene Therapy*, *23*(12), 1237–1246. https://doi.org/10.1089/hum.2012.029

Sáenz-Cuesta, M., Irizar, H., Castillo-Triviño, T., Muñoz-Culla, M., Osorio-Querejeta, I., Prada, A., Sepúlveda, L., López-Mato, M. P., López de Munain, A., Comabella, M., Villar, L. M., Olascoaga, J., & Otaegui, D. (2014). Circulating microparticles reflect treatment effects and clinical status in multiple sclerosis. *Biomarkers in Medicine*, *8*(5), 653–661. https://doi.org/10.2217/bmm.14.9

Shurtleff, M. J., Yao, J., Qin, Y., Nottingham, R. M., Temoche-Diaz, M. M., Schekman, R., & Lambowitz, A. M. (2017). Broad role for YBX1 in defining the small noncoding RNA composition of exosomes. *Proceedings of the National Academy of Sciences of the United States of America*, *114*(43), E8987–E8995. https://doi.org/10.1073/pnas.1712108114

Statello, L., Maugeri, M., Garre, E., Nawaz, M., Wahlgren, J., Papadimitriou, A., Lundqvist, C., Lindfors, L., Collén, A., Sunnerhagen, P., Ragusa, M., Purrello, M., Di Pietro, C., Tigue, N., & Valadi, H. (2018). Identification of RNA-binding proteins in exosomes capable of interacting with different types of RNA: RBP-facilitated transport of RNAs into exosomes. *PLoS ONE*, *13*(4), e0195969. https://doi.org/10.1371/journal.pone.0195969

Turchinovich, A., Drapkina, O., & Tonevitsky, A. (2019). Transcriptome of extracellular vesicles: State-of-the-art. *Frontiers in Immunology*, *10*, 202. https://doi.org/10.3389/fimmu.2019.00202

Urbanelli, L., Buratta, S., Sagini, K., Tancini, B., & Emiliani, C. (2016). Extracellular vesicles as new players in cellular senescence. *International Journal of Molecular Sciences*, *17*(9), 1408. https://doi.org/10.3390/ijms17091408

Valadi, H., Ekström, K., Bossios, A., Sjöstrand, M., Lee, J. J., & Lötvall, J. O. (2007). Exosome-mediated transfer of mRNAs and microRNAs is a novel mechanism of genetic exchange between cells. *Nature Cell Biology*, *9*(6), 654–659. https://doi.org/10.1038/ncb1596

Villarroya-Beltri, C., Gutiérrez-Vázquez, C., Sánchez-Cabo, F., Pérez-Hernández, D., Vázquez, J., Martin-Cofreces, N., Martinez-Herrera, D. J., Pascual-Montano, A., Mittelbrunn, M., & Sánchez-Madrid, F. (2013). Sumoylated hnRNPA2B1 controls the sorting of miRNAs into exosomes through binding to specific motifs. *Nature Communications*, *4*, 2980. https://doi.org/10.1038/ncomms3980

Vlassov, A. V., Magdaleno, S., Setterquist, R., & Conrad, R. (2012). Exosomes: Current knowledge of their composition, biological functions, and diagnostic and therapeutic potentials. *Biochimica et Biophysica Acta*, *1820*(7), 940–948. https://doi.org/10.1016/j.bbagen.2012.03.017

Voznyi, Y., Karpova, E. A., Dudukina, T. V., Tsvetkova, I. V., Boer, A. M., Janse, H. C., & van Diggelen, O. P. (1993). A fluorimetric enzyme assay for the diagnosis of Sanfilippo disease C (MPS III C). *Journal of Inherited Metabolic Disease*, *16*(2), 465–472. https://doi.org/10.1007/BF00710299

Weismann, C. M., Ferreira, J., Keeler, A. M., Su, Q., Qui, L., Shaffer, S. A., Xu, Z., Gao, G., & Sena-Esteves, M. (2015). Systemic AAV9 gene transfer in adult GM1 gangliosidosis mice reduces lysosomal storage in CNS and extends lifespan. *Human Molecular Genetics*, *24*(15), 4353–4364. https://doi.org/10.1093/hmg/ddv168

Wu, B., Su, S., Patil, D. P., Liu, H., Gan, J., Jaffrey, S. R., & Ma, J. (2018). Molecular basis for the specific and multivariant recognitions of RNA substrates by human hnRNP A2/B1. *Nature Communications*, *9*(1), 420. https://doi.org/10.1038/s41467-017-02770-z

Yanshina, D. D., Kossinova, O. A., Gopanenko, A. V., Krasheninina, O. A., Malygin, A. A., Venyaminova, A. G., & Karpova, G. G. (2018). Structural features of the interaction of the 3'-untranslated region of mRNA containing exosomal RNA-specific motifs with YB-1, a potential mediator of mRNA sorting. *Biochimie*, *144*, 134–143. https://doi.org/10.1016/j.biochi.2017.11.007

SUPPORTING INFORMATION

Additional supporting information can be found online in the Supporting Information section at the end of this article.

How to cite this article: Bobo, T. A., Robinson, M., Tofade, C., Sokolski-Papkov, M., Nichols, P., Vorobiov, S., & Fu, H. (2024). AAV gene replacement therapy for treating MPS IIIC: Facilitating bystander effects via EV-mRNA cargo. *Journal of Extracellular Vesicles*, *13*, e12464. https://doi.org/10.1002/jev2.12464